(1)

OFFICE OF NAVAL RESEARCH

Research Contract N00014-91-J-1909

R&T Code 4133035

Program Manager Robert J. Nowak

Technical Report No. 3

"Hydrogen Bonding and Molecular Orientation in Water/Fluorine Adlayers on Silver(110)"

by

A. Krasnopoler, A. L. Johnson, and E. M. Stuve

Prepared for Publication

in

Surface Science

Department of Chemical Engineering, BF-10
University of Washington
Seattle, WA 98195

July, 1994

REPORT DOCUMENTATION PAGE

Form Approved
OMB No. 0704-0188

1. AGENCY USE ONLY *(Leave Blank)*	2. REPORT DATE	3. REPORT TYPE AND DATES COVERED
	11 July 1994	6/94 – 5/95

4. TITLE AND SUBTITLE

Hydrogen Bonding and Molecular Orientation in Water/Fluorine Adlayers on Silver(110)

5. FUNDING NUMBERS

N00014-91-J-1909

R&T Code 4133035

Robert J. Nowak

6. AUTHOR(S)

A. Krasnopoler, A. L. Johnson, and E. M. Stuve

7. PERFORMING ORGANIZATION NAME(S) AND ADDRESS(ES)

Department of Chemical Engineering, BF-10
University of Washington
Seattle, WA 98195

8. PERFORMING ORGANIZATION REPORT NUMBER

Technical Report No. 3

9. SPONSORING / MONITORING AGENCY NAME(S) AND ADDRESS(ES)

Office of Naval Research
800 N. Quincy Street
Arlington, VA 22217

10. SPONSORING/MONITORING AGENCY REPORT NUMBER

11. SUPPLEMENTARY NOTES

12a. DISTRIBUTION / AVAILABILITY STATEMENT

This document has been approved for public release and sale; its distribution is unlimited.

12b. DISTRIBUTION CODE

13. ABSTRACT *(Maximum 200 words)*

The orientation and hydrogen bonding interactions of water coadsorbed with atomic fluorine on Ag(110) were examined with high resolution electron energy loss spectroscopy (HREELS) and time-of-flight measurements of electron stimulated desorption ion angular distribution (TOF-ESDIAD). Water exhibits four stabilized adsorption states in the presence of fluorine, identified as the B, A_1, A_2, and A_3 states in order of their decreasing desorption temperatures. The B state interacts with fluorine through one hydrogen bond with the other hydrogen remaining free as evidenced by an O–H stretching frequency of 3700 cm^{-1}. Water molecules in the A_1 state interact through two strong hydrogen bonds in a ratio of one water molecule per fluorine atom and cause a (2x1) to (1x2) surface phase transition of fluorine. Surprisingly, TOF-ESDIAD measurements detect no H^+ emission from either the B or A_1 states indicating that all hydrogens are either pointed towards the surface or far enough away from the surface normal to escape detection by ESDIAD. Instead, emission of only high mass ions ($O^+/OH^+/H_2O^+/F^+$) occurs in two beams along the [$\bar{1}$10] direction for the B state and along the [001] direction for the combined B + A_1 states. The A_2 and A_3 states of water hydrogen bond to the B and A_1 states and exhibit vibrational spectra that approach that of ice, although the interaction with fluorine remains sufficiently strong to impart measurable spectral differences.

14. SUBJECT TERMS

Double Layer Modeling, Solvation, Fluorine Adsorption, Water Adsorption, Metal/Electrolyte Interface

15. NUMBER OF PAGES

29

16. PRICE CODE

17. SECURITY CLASSIFICATION OF REPORT	18. SECURITY CLASSIFICATION OF THIS PAGE	19. SECURITY CLASSIFICATION OF ABSTRACT	20. LIMITATION OF ABSTRACT
Unclassified	Unclassified	Unclassified	

HYDROGEN BONDING AND MOLECULAR ORIENTATION IN WATER/FLUORINE ADLAYERS ON SILVER(110)

A. Krasnopoler, A. L. Johnson, and E. M. Stuve*

Department of Chemical Engineering, BF-10

University of Washington

Seattle, Washington 98195, USA

Submitted to

Surface Science

July, 1994

*Address correspondence to this author.

ABSTRACT

The orientation and hydrogen bonding interactions of water coadsorbed with atomic fluorine on Ag(110) were examined with high resolution electron energy loss spectroscopy (HREELS) and time-of-flight measurements of electron stimulated desorption ion angular distribution (TOF-ESDIAD). Water exhibits four stabilized adsorption states in the presence of fluorine, identified as the B, A_1, A_2, and A_3 states in order of their decreasing desorption temperatures. The B state interacts with fluorine through one hydrogen bond with the other hydrogen remaining free as evidenced by an O–H stretching frequency of 3700 cm^{-1}. Water molecules in the A_1 state interact through two strong hydrogen bonds in a ratio of one water molecule per fluorine atom and cause a (2x1) to (1x2) surface phase transition of fluorine. Surprisingly, TOF-ESDIAD measurements detect no H^+ emission from either the B or A_1 states indicating that all hydrogens are either pointed towards the surface or far enough away from the surface normal to escape detection by ESDIAD. Instead, emission of only high mass ions ($O^+/OH^+/H_2O^+/F^+$) occurs in two beams along the $[\bar{1}10]$ direction for the B state and along the [001] direction for the combined B + A_1 states. The A_2 and A_3 states of water hydrogen bond to the B and A_1 states and exhibit vibrational spectra that approach that of ice, although the interaction with fluorine remains sufficiently strong to impart measurable spectral differences.

1. INTRODUCTION

This work continues our investigation [1] of water coadsorbed with fluorine on Ag(110) as part of an effort to study surface solvation and its influence at the electrochemical interface. Obtaining an accurate depiction of surface solvated ion structure has acquired a renewed urgency because of recent x-ray scattering measurements that reveal unusually dense surface water at Ag(111) electrodes in NaF electrolyte [2]. Surface water densities nearly twice that of ice Ih occur at potentials positive of the potential of zero charge (PZC), implicating the influence of adsorbed fluoride in establishing such adlayers. A recent far-infrared study [3] of Ag(111) in NaF electrolyte did not observe a direct influence of adsorbed fluoride, although the amount of adsorbed water increases at potentials progressively more negative of the PZC, presumably because of the desorption of fluoride.

Recent calculations have shown that fluoride ion in solution has a hydration shell consisting of an average of 17.4 water molecules divided into primary and secondary shells of 6.0 and 11.4 water molecules, respectively [4]. That study, which implemented a charged, hard-wall electrode, found no specific adsorption (also known as contact adsorption) of fluoride, in contrast to the experimental findings of specifically adsorbed fluoride at silver electrodes [5]. Nonetheless, the calculations showed that fluoride in its nonspecifically adsorbed form causes water to interact with the surface through the hydrogen atoms, whereas surface science studies typically propose interaction through the oxygen atom [6,7].

Simulation of the electrochemical double layer by adsorbing water on a fluorine-covered Ag(110) surface in ultrahigh vacuum (UHV) provides a route to an experimentally derived, molecular-level understanding of the interactions among fluorine, water, and a silver surface. The ability of this methodology to

mimic qualitative and certain quantitative details of the real electrochemical surface has been established [8-11], and a good literature base for studies of the structure of water at metal surfaces [7,12-20] and the influence of coadsorbed ions [1,7,9-11,21-26] now exists. As previously reported [1,27], fluorine is hydrated by water in four states classified on the basis of thermal desorption temperatures: the B state, which desorbs at 230 - 270 K; the A_1 state at 220 K; the A_2 state at 190 K; and the A_3 state at 175 K. (Multilayer water desorbs at 160 K.) For fluorine coverages greater than 0.2 ML, the B and A_1 states consist of, respectively, 0.5 ± 0.25 and 1 ± 0.2 water molecules per fluorine atom [27]. The total surface hydration number (all states) varies from 14 in the limit of zero fluorine coverage to 2 at coverages above 0.4 ML. The larger number agrees well with the calculations mentioned above and supports the existence of primary and secondary hydration shells in the case of specific adsorption. In terms of its surface hydration characteristics, adsorbed fluorine behaves as F^-, as the energetics of fluorine surface hydration strongly resemble those for hydration of single fluoride ions in the gas phase.

The present work combines the results of high resolution electron energy loss spectroscopy (HREELS) and time-of-flight measurements of electron stimulated desorption ion angular distribution (TOF-ESDIAD) with the previous results to elucidate adsorption models for the most strongly hydrating water molecules of fluorine on Ag(110). The nature and extent of hydrogen bonding is determined by comparison of the HREELS vibrational spectrum of adsorbed water with infrared and Raman spectra of ice and gas phase water [28-30], listed in Table 1. ESDIAD measurements provide information about the orientation of adsorbed water molecules [1,7,14,21,24,31,32] and, when coupled with time-of-flight measurements, allow a distinction of H^+ from the higher mass ions

$O^+/OH^+/H_2O^+/F^+$. When combined with other surface science measurements, the real space ESDIAD images often provide critical information in selecting one of the possible bonding models identified by the other techniques.

2. EXPERIMENTAL PROCEDURE

The experiments were conducted in a stainless steel UHV chamber that has been described previously [23,26]. The typical resolution (full width at half-maximum, FWHM) of the electron energy loss spectra was 100 cm^{-1}, and all energy losses are rounded to the nearest 5 cm^{-1}. Time-of-flight detection of positive ions in ESDIAD was accomplished with a pulsed, incident electron beam and a gating voltage applied to the last hemispherical and flat grids of the ESDIAD optics. The gating voltage was timed to allow ion transmission to the microchannel plates only for a given period of time after the electron gun pulse [31]. The transit times for H^+ and F^+ from sample to detector were approximately 300 and 1500 ns, respectively. The gate width of 100 ns allowed distinction of H^+ from higher mass ions, but O^+, OH^+, H_2O^+, and F^+ could not be unambiguously resolved from each other. The energy of the electrons incident on the sample was 300 eV and the sample was biased 60 V positive of the ESDIAD optics. All coverages are reported in units of monolayers (ML), where 1 ML represents a 1:1 ratio of adsorbate to topmost Ag(110) surface atoms, or 8.45 x 10^{14} cm^{-2}. Details of substrate and adsorbate preparation have been published previously [1].

3. RESULTS

Atomic fluorine was generated on the Ag(110) surface by coadsorption of O_2 and HF at 100 K followed by heating to 400 K. The ensuing surface reaction

produces H_2O and adsorbed atomic F, as previously discussed [1]. The use of adsorbed molecular oxygen as the reactant in this work, as opposed to adsorbed atomic oxygen in the earlier study, caused no detectable differences in the behavior of coadsorbed H_2O and F.

Electron energy loss spectra of varying amounts of H_2O coadsorbed with 0.3 ML of F are shown in fig. 1. These data were obtained following adsorption of multilayers of H_2O on the F-covered surface at 100 K and annealing to successively higher temperatures to isolate the individual adsorption states of water. The actual state of adsorbed water was verified by TDS immediately following the HREELS measurements, as shown in fig. 2. The TDS results illustrate the distribution of water in the four stabilized states and provide a more accurate characterization of the adsorbate than simply stating an annealing temperature. For the lowest water coverage, which corresponds to the B state, the energy loss spectrum shows a peak at 3700 cm^{-1} characteristic of a nonhydrogen bonded O–H stretching mode ν(OH). (Table 1 lists peak positions and assignments in comparison with gaseous and solid water.) This peak becomes included in a broad band and shifts slightly to higher energy when both A_1 and B states are present. The portion of the ν(OH) band attributable to the A_1 state, that is, exclusive of the high energy peak at 3720 cm^{-1}, is centered at 3385 cm^{-1}. Increasing the water coverage to include the A_2 state gives two distinct ν(OH) peaks at 3305 and 3670 cm^{-1}. When all four states are present, the ν(OH) region exhibits a relatively intense, broad peak centered at 3280 cm^{-1} with a small, high energy peak at 3665 cm^{-1}.

The broad δ band representing the H–O–H scissoring mode for the B state is composed of two peaks at 1460 and 1615 cm^{-1}. As the lowest scissoring energies reported for adsorbed water fall in the range of 1575 to 1595 cm^{-1} [13,15,16,20],

the 1460 cm^{-1} peak most likely represents an overtone of the 775 cm^{-1} librational band. Thus, the 1615 cm^{-1} peak is assigned to the scissoring mode of water in the B state. This band shifts up in energy to 1670 cm^{-1} when both the B and A_1 states are present. When all four states are present it shifts down in energy to 1635 cm^{-1}, in good agreement with the scissoring mode for H_2O ice. The librational modes (ρ) of the B state appear in a relatively sharp band at 775 cm^{-1}. This band splits into two components at 710 and 875 cm^{-1} with the addition of the A_1 state. Increasing the water coverage to include the A_2 and A_3 states produces an asymmetrical libration band with the peak located at 905 cm^{-1}. The $\tau/\nu(AgX)$ peak includes contributions from frustrated translations (τ) of ice, the Ag–F stretching mode $\nu(AgF)$, and the Ag-water stretching mode $\nu(AgO)$. It appears at 320 cm^{-1} when only the B state of H_2O and atomic F are present, and shifts progressively to lower energy upon addition of water, ending up at 270 cm^{-1} when all four states of water are present.

Fig. 3 shows energy loss spectra for D_2O coadsorbed with atomic F. The $\nu(OD)$ region for the B state (curve (a)) exhibits two distinct peaks at 2380 and 2725 cm^{-1}. The higher and lower energy peaks correspond to nonhydrogen bonded and hydrogen bonded O-D stretching modes, respectively. The hydrogen bonded peak indicates that a small amount of D_2O in the A_1 state was present for this spectrum, as seen by comparison with curve (b) for the combined B + A_1 states. The peak at 2655 cm^{-1} in fig. 3(b) extends to sufficiently high energy loss to indicate that a free O-H strectch is also present for the B + A_1 states. The scissoring mode shifts up in energy from 1185 cm^{-1} for the B state to 1210 cm^{-1} when the B, A_1, and A_2 states are present. Likewise, the librational band shifts to higher energy with increasing water coverage, from 585 cm^{-1} for the B state to 650 cm^{-1} for the B + $A_{1,2}$ states. Although two features were

observed in the librational band for the B + A_1 states of H_2O, only one feature with a maximum at 605 cm^{-1} was resolved for D_2O. The τ/ν(AgX) peak of D_2O is similar to that of H_2O, exhibiting a similar shift to lower energy with increasing D_2O content on the surface.

Mass resolved ESDIAD patterns were obtained from a variety of water coverages on the F-covered surface. Adsorbed, atomic fluorine alone produced F^+ emission in two primary beams oriented along the [1$\bar{1}$0] direction, as shown in the contour plot of fig. 4(a). The same pattern occurred for the B state of water coadsorbed with fluorine. When both B and A_1 states were present the pattern changed to that shown in fig. 4(b) with two beams oriented along the [001] direction. A superposition of the two patterns in fig. 4 occurred when the B state and a partially filled A_1 state were present. Surprisingly, both patterns were composed of only high mass ions $O^+/OH^+/H_2O^+/F^+$; there was no detectable H^+ emission. H^+ emission is typical for adsorbed H_2O and is easily detected, for example, when H_2O multilayers are present.

4. DISCUSSION

4.1 Model of the B State for H_2O/F/Ag(110)

Examination of the vibrational energies in Table 1 reveals that increasing water content on the fluorine-covered surface causes a general progression from an incompletely hydrogen bonded (B state) to a fully hydrogen bonded adsorbate (B + $A_{1,2,3}$ states). The ν(OH) and ν(OD) peaks at 3700 and 2725 cm^{-1} for the B state are in excellent agreement with the uncoupled, nonhydrogen bonded O–H and O–D stretching modes of HDO. However, some hydrogen bonding is present as seen by the increased energy of the scissoring mode (1615 cm^{-1}) compared to that for gaseous water (1595 cm^{-1}). Hydrogen bonding

increases the energy of the scissoring mode by increasing the force constant against motion of the H atoms perpendicular to the hydrogen bond axis. The reduction of the scissoring energy compared to that of ice (1650 cm^{-1}) indicates that hydrogen bonding is not as strong in the B water molecule as in ice. Furthermore, the scissoring energy is consistent with vibrational calculations of water linearly bonded to F^-, which show a reduction in the bending force constant from that of ice without perturbation of the force constant for the free O–H stretch [33]. The librational band at 775 cm^{-1} is lower in energy than ice librations, but is unusually intense given the relatively small amount of B molecules on the surface (0.1-0.2 ML). The τ/ν(AgX) mode at 320 cm^{-1} represents either the Ag–F or Ag–OH_2 stretches (or both). It is in excellent agreement with a band at 322 cm^{-1} attributed to ν(Ag–OH_2) for Ag(111) in 0.1 M NaF at room temperature, as well as the estimate of ν(AgF) of 325 cm^{-1} [3].

Since only one O–H stretching mode was detected, we conclude that the two O–H bonds become inequivalent upon interaction with F. In the extreme, this inequivalence could result from a chemical reaction to HF and OH. Such a reaction can be ruled out on the basis of TDS results [1] and vibrational spectroscopy. H–F stretches occur at 3110 and 3370 cm^{-1} for anhydrous HF on Pt(111) [22], and ν(OH) of OH groups on Ag(110) occurs at 3380 cm^{-1} [12]. Infrared measurements of HF and H_2O in rare gas lattices detect ν(HF) of monomers and dimers above 3800 cm^{-1}, whereas modes between 3700 and 3800 cm^{-1} are due to H_2O [34].

Figure 5 shows a model of H_2O in the B state derived from the LEED [1], HREELS, and ESDIAD results. The fluorine atoms are arranged in a p(2x1) structure and located in the trough at asymmetric bridge sites in accord with the ESDIAD results of fig. 4(a) and chemical intuition favoring high coordination of

the adatom. Since the number of B water molecules per fluorine atom is less than unity [27], water molecules must be located randomly about the surface, as opposed to occupying a distinct position within a perfect (2x1) unit cell. One of the inequivalent O–H bonds, the one detected by HREELS, remains nonhydrogen bonded, whereas the other interacts with fluorine in a manner that excludes detection by HREELS. The most straightforward realization of the latter result is to propose a hydrogen bonded O–H bond parallel to the surface. There are two general configurations that allow this, as shown in fig. 5. In one, the water molecule resides in the trough, with one hydrogen bond to fluorine in the $[1\bar{1}0]$ direction and the free O–H bond tilted off the surface normal to an extent that excludes its detection by ESDIAD. Reneutralization occurs for protons emitted at angles greater than 50-60° from the surface normal [32], so an O–H bond tilted at least this much will not display an H^+ signal in ESDIAD. This configuration is similar to those proposed for the H_2O/Br [35] and H_2O/Cl [25] coadsorption systems on Ag(110).

In the other possible configuration, shown in the hatched box, water resides atop a ridge atom, with one bent hydrogen bond to fluorine and the free O–H bond again tilted more than 60° away from the surface normal. This configuration is proposed on the basis of calculations that show water should adsorb at atop sites [6]. The metal/water interaction most likely occurs through one of the two lone pairs of electrons on the oxygen atom which are located at tetrahedral positions with respect to the hydrogen atoms. The model in the hatched box allows one lone pair to interact directly with an atop silver atom, an interaction that should be favored by the electron withdrawing character of the adjacent fluorine atom and lead to an unusually strongly adsorbed state. Note that an atop configuration with both hydrogens interacting with fluorine atoms

would not allow overlap of the oxygen lone pair with any silver atom and would also conflict with the HREELS finding of a free O–H bond.

Either model of the B state has C_s symmetry in agreement with *ab initio* self consistent field calculations [36], molecular dynamics calculations [37], and infrared spectroscopy of dilute HDO in fluoride solutions [38]. However, a C_{2v} structure was proposed for H_2O interacting with gas phase F^- in which *both* hydrogens interact with fluorine [39]. Nuclear magnetic resonance studies of aqueous fluoride solutions also favored a C_{2v} symmetry [40]. The HREELS results clearly detect a nonhydrogen bonded O–H moiety, thereby ruling out a C_{2v} structure.

4.2 Model of the A_1 State

A structural model for the A_1 state must conform to the following results.

(i) The vibrational spectrum of the B + A_1 state exhibits a peak characteristic of a free (nonhydrogen bonded) O–H stretching mode.

(ii) A band characteristic of hydrogen bonded O–H stretching modes appears in the vibrational spectrum of the B + A_1 state. Hydrogen bonding is also evident in the librational and scissoring peaks of the vibrational spectrum.

(iii) For fluorine coverages greater than 0.2 ML, the LEED pattern changes from p(2x1) for fluorine alone to p(1x2) for the B + A_1 state [1].

(iv) The ratio of A_1 water molecules to fluorine atoms is 1 ± 0.2 [27].

(v) The primary azimuthal direction for ESDIAD emission changes from $[1\bar{1}0]$ (for fluorine adsorbed either alone or with the B state) to [001] for the B + A_1 state. There is no H^+ emission in any of these cases.

Figure 6 shows a model of the B + A_1 state of water interacting with adsorbed

fluorine. Before discussing this model, we must point out that one of the problems with any "billiard ball" model of this type is that it often conveys more information than is known about the system. This particular model is not necessarily unique; variations ranging from minor (for example, shifting the A_1 molecules from the left side of the fluorine atoms to the right side) to major may exist. Nonetheless, we believe this model to be the simplest one that fits all of the available data and will limit its discussion to what is known about the system.

From point (i) we can infer that the free O–H bond of the B molecule remains free when the A_1 molecules are present. The broad band in the hydrogen bonded O–H stretching region (figs. 1(b) and 3(b)) signifies that both hydrogen atoms of the A_1 molecule participate in strong hydrogen bonding, in agreement with point (ii). These hydrogens are directed toward the surface (or far enough away from the surface normal) so as to avoid detection as H^+ by ESDIAD, as specified in point (v). The blue-shifted energy of the scissoring mode of 1670 cm^{-1} (1205 cm^{-1} for D_2O) indicates that the A_1 scissoring force constant meets or exceeds that of ice. This can arise from a combination of water-metal interactions and hydrogen bonding and is consistent with the relatively high desorption temperature (220 K) of the A_1 state. A similar combination of water-metal interactions and hydrogen bonding has been proposed to explain the high peak [temperature of 260 K for water desorption from Ni(110) [41].

The (2x1) to (1x2) transition stated in point (iii) indicates a rearrangement of the adatoms on the surface. We rule out the possibility of a reconstruction on the grounds that as alkali adsorption causes a (1x2) reconstruction on Ag(110) [42], halogen adsorption, with its opposite charge transfer, is unlikely to produce the same reconstruction. The (2x1) to (1x2) transition attests to movement of fluorine on the surface, so we assign the (1x2) pattern to adsorbed fluorine in the presence

of the B + A_1 state. Comparison of figs. 5 and 6 shows that this transition can occur by movement of the fluorine atoms in the $[\bar{1}10]$ direction in such a manner that fluorines in adjacent troughs move in opposite directions. This avoids the energetically unfavorable pathway whereby fluorine atoms diffuse across the ridges in the [001] direction. In going from the model of fig. 5 to that of fig. 6, the largest movement by any fluorine atom is two lattice constants. This produces antiphase domains, but as the displacement vector is one substrate lattice constant in each direction, spot splitting does not occur in the LEED pattern.

Each (1x2) unit cell contains one A_1 molecule, as specified by point (iv), whereas the B molecules cannot occupy a regular part of the (1x2) unit cell on account of the B/F ratio of 0.5 discussed above. We propose that the B molecules remain largely as depicted in either configuration of fig. 5, except that they move with the fluorine atoms during the (2x1) to (1x2) transition and interact with fluorines located at the edges of (1x2) domains, as shown in fig. 6. The B/F ratio, which is exactly 0.5 in fig. 6, depends on the size of the (1x2) domains. Larger domains yield ratios less than 0.5 and become increasingly unlikely as they require fluorine movement over much larger distances to accomplish the (2x1) to (1x2) transition. Smaller domains yield ratios greater than 0.5, but would be almost unrecognizable by LEED. Of course, one expects a distribution of domain sizes and, consequently, a distribution in the B/F ratio, which again agrees with the TDS results [27].

The TOF-ESDIAD results of point (v) provide information about the intra-unit cell structure of the B + A_1 model. The absence of H^+ emission for both the B and the B + A_1 states means that no O–H bond orients with the hydrogen pointing away from the surface within about 50° of the surface normal [32]. Unfortunately, the time-of-flight detector used in these experiments could not

resolve which of the possible ions, $O^+/OH^+/H_2O^+/F^+$, produces the ESDIAD pattern. Beginning with F^+ as a possibility, we note that the absence of emission along $[1\bar{1}0]$ for the A_1 state indicates a shift of fluorine out of the asymmetric trough site. We therefore propose the three-fold, (111)-like site shown in fig. 6 which would produce the corresponding ESDIAD signal along the [001] direction should F^+ be the ion source. Another possible ESDIAD source is H_2O^+ resulting from electron stimulated rupture of the metal-water bond, as also indicated in fig. 6. For this possibility to occur, the influence of the hydrogen bonds to the fluorine atoms would have to be minimal; at present we have no way of knowing whether that is the case. Emission of OH^+, an *a priori* possibility, requires at least one O–H bond oriented in the [001] direction. However, we have been unable to find a model that allows for OH^+ emission and that conforms to all of the previously discussed data, and therefore discount the possibility of OH^+ as the ion source. Likewise, we eliminate O^+ as a source as that route would require the unlikely event of breaking two O–H bonds in a single electron scattering event. In light of this discussion, it is clear that better mass resolved ESDIAD measurements are required for accurate identification of the desorbing ion.

As in our previous study [1], we compare the model of fig. 6 with the H_2O/OH [21] and H_2O/Cl [25] coadsorption systems on Ag(110). The (1x2) unit cell and three-fold adsorption site for fluorine are the same as those proposed for OH on Ag(110), which is reasonable in that fluorine is isoelectronic with OH. Furthermore, the B + A_1 state shares many similarities with the γ H_2O/OH state. Both systems have similar ESDIAD patterns and desorption peak temperatures (220 K). The proposed orientation and hydrogen bonding interactions of the A_1 and γ water molecules are essentially the same. The only differences between the

two are (1) that the ratio of γ water molecules to OH is 0.5, as compared to 1 for the A_1/F ratio, and (2) that the proposed adsorption site for OH is atop a trough atom in the γ state, as opposed to the three-fold site for fluorine.

The ability of coadsorbed water to induce movement of fluorine atoms parallels that for coadsorbed water and chlorine [25]. The latter surface hydration system exhibits a p(4x3) structure for chlorine coverages between 0.25 and 0.4 and a c(4x4) structure for chlorine coverages of 0.4 to 0.5. In that case, removal of water by thermal desorption allows chlorine to return to its natural p(2x1) structure (also similar to fluorine). We attribute the ability of water to cause large surface movements of these strongly bound halogens as the result of dielectric screening in which proximate water moleules screen the negative charge of the halogen. In the previous paper [1], we demonstrated the quantitative parallels between surface hydration of adsorbed fluorine and gas phase hydration of fluoride ion, and calculations [43] also support interpretation of adsorbed fluoride as a negatively charged species.

4.3 Hydrogen Bonding in the A_1, A_2, and A_3 States

As previously noted, the increased scissoring energy of the A_1 state exceeds that of ice and signifies stronger hydrogen bonding than in ice [7,20]. Essentially the same conclusion can be reached upon examination of the librational band [20]. The energy of the 875 cm^{-1} peak also exceeds that of ice, indicating that the A_1 molecules experience an increase in at least one of the librational force constants brought about by stronger hydrogen bonding. The lower energy shoulder suggests that the other librations have weaker force constants than those of ice, which is consistent with water molecules interacting with fewer than four other water molecules [20].

As depicted in fig. 6, the hydrogen bond between the A_1 molecule and fluorine (O–H···F) is 150°. This bond angle follows from the use of an O–F distance of 0.26 nm in accord with the calculated results of hydrated fluoride ion in solution [4]. (The equilibrium O–O distance in ice at 193 K is 0.275 nm [30].) Hydrogen bonds are normally assumed to be linear, though deviations from linearity of as much as 25° may occur with no change in bond strength [44]. At higher angles of nonlinearity the bond progressively weakens, and at 30°, the decrease in the hydrogen bond strength between two water molecules has been estimated as 15% [44]. The A_1 configuration shown in fig. 6 therefore allows reasonably strong hydrogen bonding along with a favorable geometry for overlap of the A_1 lone pair electrons with a ridge substrate atom.

With the addition of the A_2 and A_3 states of water, the vibrational spectra show an increasing number of water molecules involved in hydrogen bonding. The OH stretching region broadens and shifts to lower energy with a maximum at 3280 cm^{-1} due to hydrogen bonding. The small peak at 3665 cm^{-1} could be due to interactions between the B and A states causing a small decrease in vibrational energy, or to free OH stretches within the second layer of water. The scissoring mode shifts back down to 1635 cm^{-1}, slightly below that of ice, whereas the higher energy librational peak shifts up to 905 cm^{-1}, greater than the energy of ice librations. In comparison, the $\delta(H_2O)$ and $\rho(H_2O)$ peaks occur at 1660 and 810 cm^{-1}, respectively, for a similar coverage of water on clean Ag(110) [5]. These seemingly conflicting results simply mean that some aspect of the intermolecular hydrogen bonding is stronger than its equivalent in ice, whereas the other aspects are comparable or weaker than those in ice. Regardless of the exact nature of these interactions, the ability of fluorine to cause some degree of structural rearrangement on even the most weakly stabilized water molecules

(A_2 and A_3) can be readily detected with vibrational spectroscopy.

5. CONCLUSIONS

Water interacts both strongly and weakly with atomic fluorine on Ag(110). In its most strongly stabilized form (the B state) the interaction with fluorine occurs through one hydrogen bond per molecule. Water molecules in the A_1 state induce a (2x1) to (1x2) transition of adsorbed fluorine and interact with fluorine through strong hydrogen bonds directed towards the surface. The respective stoichiometries of the B and A_1 states are 0.5 and 1 water molecules per fluorine atom. Additional water molecules in the A_2 and A_3 states hydrogen bond to the B + A_1 states and form structures approaching that of ice, while remaining sufficiently distinct to be detected by vibrational spectroscopy.

ACKNOWLEDGMENTS

We gratefully acknowledge the Office of Naval Research for support of this work.

REFERENCES

[1] A. Krasnopoler and E. M. Stuve, Surf. Sci. 303 (1994) 355.

[2] M. F. Toney, J. N. Howard, J. Richer, G. L. Borges, J. G. Gordon, O. R. Melroy, D. G. Wiesler, D. Yee, and L. B. Sorensen, Nature 368 (1994) 444.

[3] A. E. Russell, A. S. Lin, and W. E. O'Grady, J. Chem. Soc. Faraday Trans. 89 (1993) 195.

[4] J. N. Glosli and M. Philpott, J. Chem. Phys. 98 (1993) 9995.

[5] M. Bacchetta, S. Trasatti, L. Doubova, and A. Hamelin, J. Electroanal. Chem. 255 (1988) 237.

[6] S.-B. Zhu and M. R. Philpott, J. Chem. Phys. 100 (1994) 6961.

[7] P. A. Thiel and T. E. Madey, Surf. Sci. Rep. 7 (1987) 211.

[8] K. Bange, B. Straehler, J. K. Sass, and R. Parsons, J. Electroanal. Chem. 229 (1987) 87.

[9] J. K. Sass, D. Lackey, J. Schott and B. Straehler, Surf. Sci. 247 (1991) 239.

[10] F. T. Wagner, in "Structure of Electrified Interfaces," J. Lipkowski and P. N. Ross (Eds.) (VCH Publishers, New York, 1993).

[11] E. M. Stuve and N. Kizhakevariam, J. Vac. Sci. Tech. A 11 (1993) 2217.

[12] E. M. Stuve, B. A. Sexton and R. J. Madix, Surf. Sci. 111 (1981) 11.

[13] P. A. Thiel, F. M. Hoffmann, and W. H. Weinberg, J. Chem. Phys. 75 (1981) 5556.

[14] D. Doering and T. E. Madey, Surf. Sci. 123 (1982) 305.

[15] L. Ollé, M. Salmerón, and A. M. Baró, J. Vac. Sci. Tech. A 3 (1985) 1866.

[16] M. Hock, U. Seip, I. Bassignana, K. Wagemann, and J. Küppers, Surf. Sci. 177 (1986) L978.

[17] C. Benndorf and T. E. Madey, Surf. Sci. 194 (1988) 63.

[18] B. W. Callen, K. W. Griffiths, U. Memmert, D. A. Harrington, S. J. Bushby, and P. R. Norton, Surf. Sci. 230 (1990) 159.

[19] B. W. Callen, K. Griffiths and P. R. Norton, Surf. Sci. Lett. 261 (1992) L44.

[20] R. Brosseau, M. R. Brustein, and T. H. Ellis, Surf. Sci. 280 (1993) 23.

[21] K. Bange, T. E. Madey, J. K. Sass and E. M. Stuve, Surf. Sci. 183 (1987) 334.

[22] F. T. Wagner and T. E. Moylan, Surf. Sci. 182 (1987) 125.

[23] R. Döhl-Oelze, C. C. Brown, S. Stark and E. M. Stuve, Surf. Sci. 210 (1989) 339.

[24] D. Lackey, J. Schott, B. Straehler and J. K. Sass, J. Chem. Phys. 91 (1989) 1365.

[25] N. Kizhakevariam, E. M. Stuve and R. Döhl-Oelze, J. Chem. Phys. 94 (1991) 670.

[26] N. Kizhakevariam and E. M. Stuve, Surf. Sci. 275 (1992) 223.

[27] A. Krasnopoler, M.S. Thesis, University of Washington (1992).

[28] D. Eisenberg and W. Kauzmann, "The Structure and Properties of Water," Oxford University Press (1969).

[29] J. E. Bertie and E. Whalley, J. Chem. Phys. 40 (1964) 1637.

[30] F. Franks, in "Water: A Comprehensive Treatise," Vol. 1, F. Franks (Ed.) (Plenum, New York, 1972) Chap. 4.

[31] S. A. Joyce, A. L. Johnson and T. E. Madey, J. Vac. Sci. Tech. A 7 (1989) 2221.

[32] Z. Miskovic, J. Vukanic, and T. E. Madey, Surf. Sci. 169 (1986) 405.

[33] M. Falk, H. T. Flakus and R. J. Boyd, Spectrochim. Acta. 42A (1986) 175.

[34] M. T. Bowers, G. I. Kerley and W. H. Flygare, J. Chem. Phys. 45 (1966) 3399.

[35] K. Bange, T. E. Madey, and J. K. Sass, Surface Sci. 162 (1985) 252.

[36] H. Kistenmacher, H. Popkie and E. Clementi, J. Chem. Phys. 58 (1973) 5627.

[37] E. Guàrdia and J.A. Padró, J. Phys. Chem. 94 (1990) 6049.

[38] O. Kristiansson and J. Lindgren, J. Mol. Struc. 177 (1988) 537.

[39] M. Arshadi, R. Yamdagni and P. Kebarle, J. Phys. Chem. 74 (1970) 1475.

[40] K. J. Müller and H. G. Hertz, Z. Phys. Chem. N.F. 140 (1984) 31.

[41] B. W. Callen, K. Griffiths, R. V. Kasza, M. N. Jensen, P. A. Thiel, and P. R. Norton, J. Chem. Phys. 97 (1992) 3760.

[42] R. Döhl-Oelze, E. M. Stuve, and J. K. Sass, Solid State Comm. 57 (1986) 323.

[43] P. S. Bagus and G. Pacchioni, Electrochim. Acta 36 (1991) 1669.

[44] C. N. R. Rao, in "Water: A Comprehensive Treatise," Vol. 1, F. Franks (Ed.) (Plenum, New York, 1972) Chap. 3.

Table 1.

Summary of HREELS results (cm^{-1}) for $H_2O(D_2O)$ coadsorbed with F on Ag(110) and comparison with gaseous water and ice Ih.

	Gas	$H_2O(D_2O)$/F/Ag(110)				Ice Ih
Mode	[28,30]	B	B + A_1	B + $A_{1,2}$	B + $A_{1,2,3}$	[29,30]
ν(OH)	3707[a]	3700	3720	3670	3665	
ν(OH···)[c]			3385	3305	3280	3220
ν(OD)	(2727)[b]	(2725)	(2655)			
ν(OD···)[c]		(2390)	(2380)	(2550)		(2425)
δ(H_2O)	1595	1615	1670	1630	1635	1650
δ(D_2O)	(1178)	(1185)	(1205)	(1210)		(1210)
ρ(H_2O)	—	775	710,875	890	905	840
ρ(D_2O)		(585)	(605)	(650)		(640)
τ(H_2O)/ν(AgX)[d]	—	320	290	285	270	229
τ(D_2O)/ν(AgX)[d]		(320)	(315)	(310)		(220)

[a]Uncoupled mode: ν(O–H) in HDO
[b]Uncoupled mode: ν(O–D) in HDO
[c]Hydrogen bonded
[d]X = F, O

FIGURE CAPTIONS

Fig. 1 Electron energy loss spectra for the various adsorbed states of H_2O on Ag(110) with 0.3 ML of F. Spectra were recorded at 100 K following annealing to various temperatures to isolate the adsorption states of interest (see fig. 2). The corresponding spectra and states are: (a) B; (b) B + A_1; (c) B + $A_{1,2}$; and (d) B + $A_{1,2,3}$.

Fig. 2 Thermal desorption spectra of H_2O following the corresponding HREELS measurements of fig. 1. These curves serve to identify the adsorption states of water present during the HREELS measurement.

Fig. 3 Electron energy loss spectra for varying coverages of D_2O coadsorbed with 0.4 ML of F on Ag(110). The water adsorption states were identified from subsequent thermal desorption spectra (not shown). The corresponding spectra and states are: (a) B; (b) B + A_1; and (c) B + $A_{1,2}$.

Fig. 4 Contour plots of TOF-ESDIAD images recorded for 0.3 ML of F (a) and the B + A_1 states for H_2O/F (b). The image in (a) also occurs when only the B state of H_2O is present. Both images result from high mass ions $O^+/OH^+/H_2O^+/F^+$. No emission of H^+ was detected.

Fig. 5 Model of the B state for $H_2O/F/Ag(110)$. Fluorine atoms (hatched circles) occupy asymmetric bridge sites in the troughs and form a (2x1) structure. Water molecules distributed randomly about the surface interact with fluorine atoms by hydrogen bonding and through-surface interactions. The hatched box designates an alternative configuration of the water molecule (see text). Emission of F^+ ions in the $[1\bar{1}0]$ direction (arrow) produces the ESDIAD pattern of fig. 4(a).

Fig. 6 Model of the B + A_1 state for $H_2O/F/Ag(110)$. Fluorine atoms (hatched circles) occupy three-fold, (111)-like sites in the trough and are arranged in a (1x2) structure. The A_1 molecules reside on the ridges and interact with fluorine atoms by hydrogen bonding and through-surface interactions. The B molecules interact with fluorine at the edges of (1x2) domains and remain in either configuration proposed in fig. 5. The ESDIAD pattern of fig. 4(b) results from emission of either F^+ or H_2O^+ as indicated by the arrows.

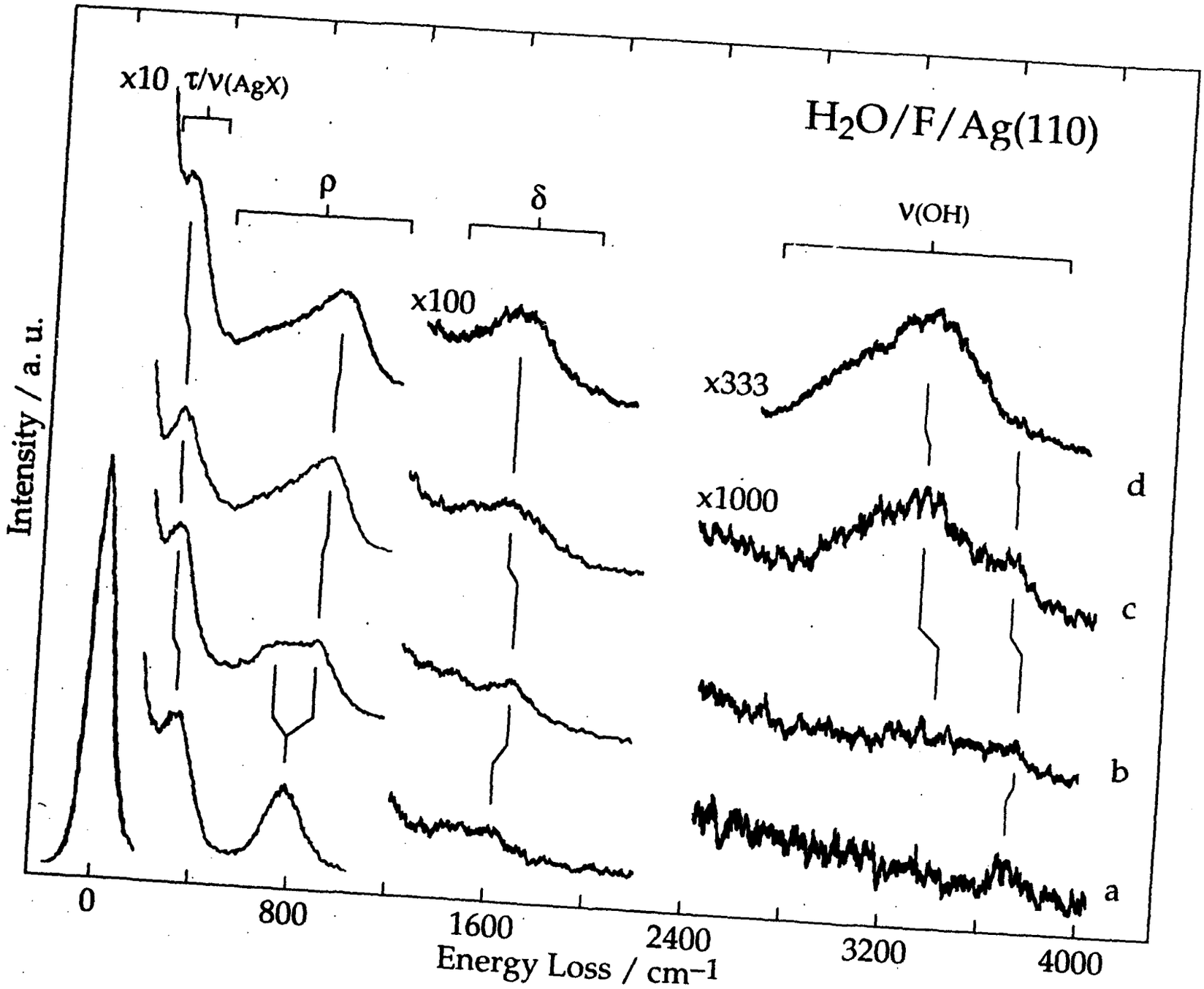

Fig. 1, Krasnopoler, Johnson, and Stuve

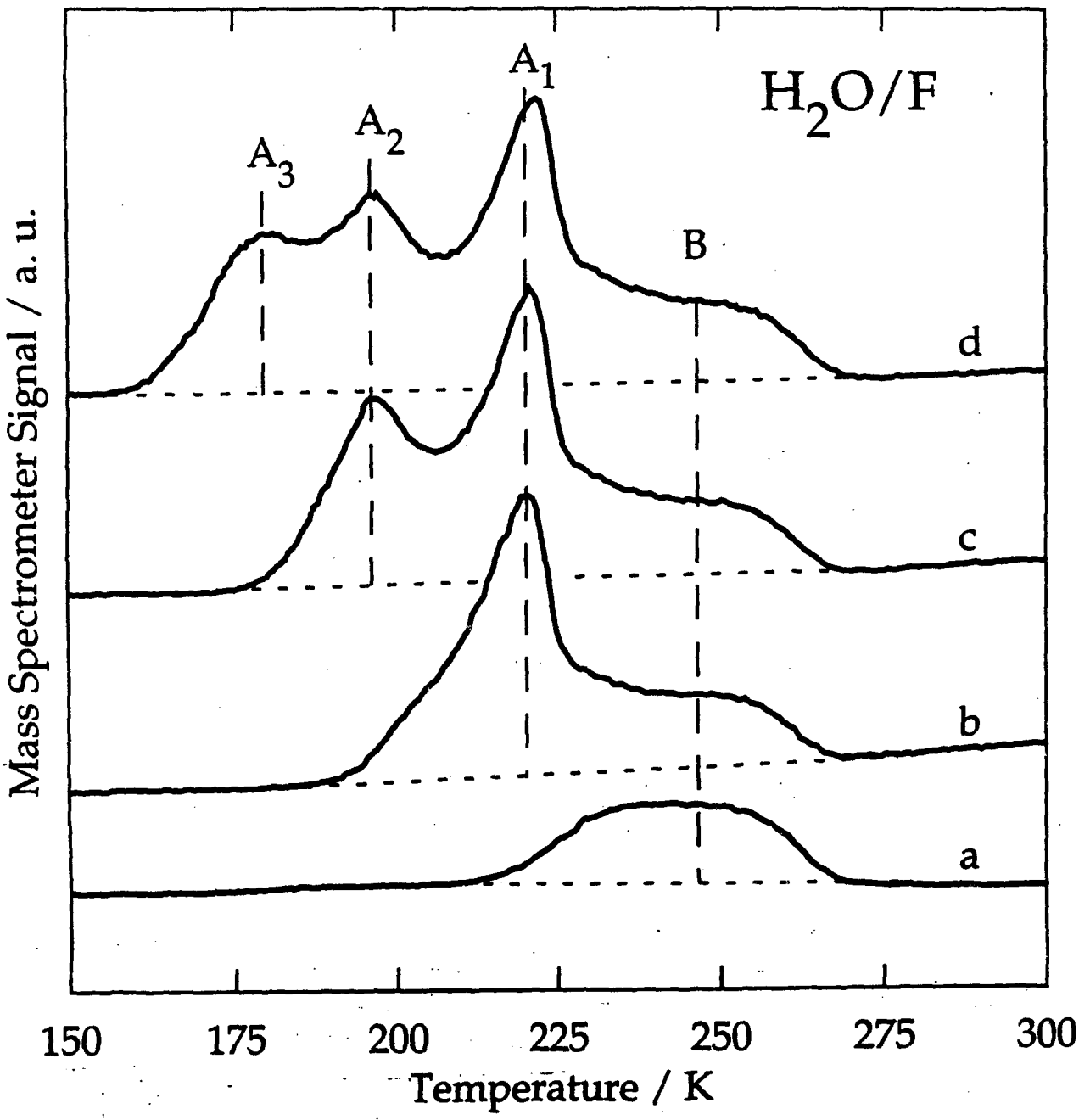

Fig. 2, Krasnopoler, Johnson, and Stuve

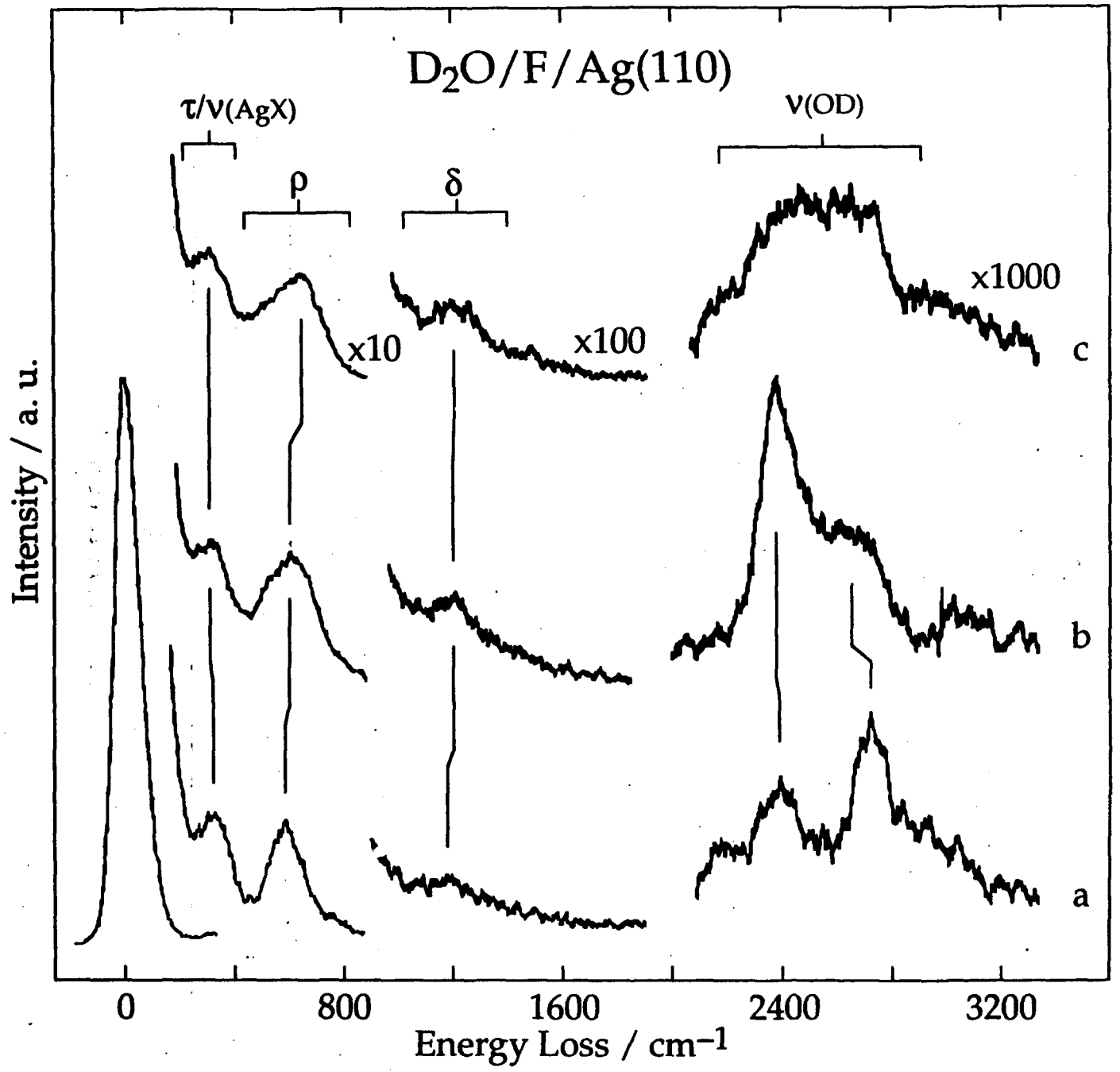

Fig. 3, Krasnopoler, Johnson, and Stuve

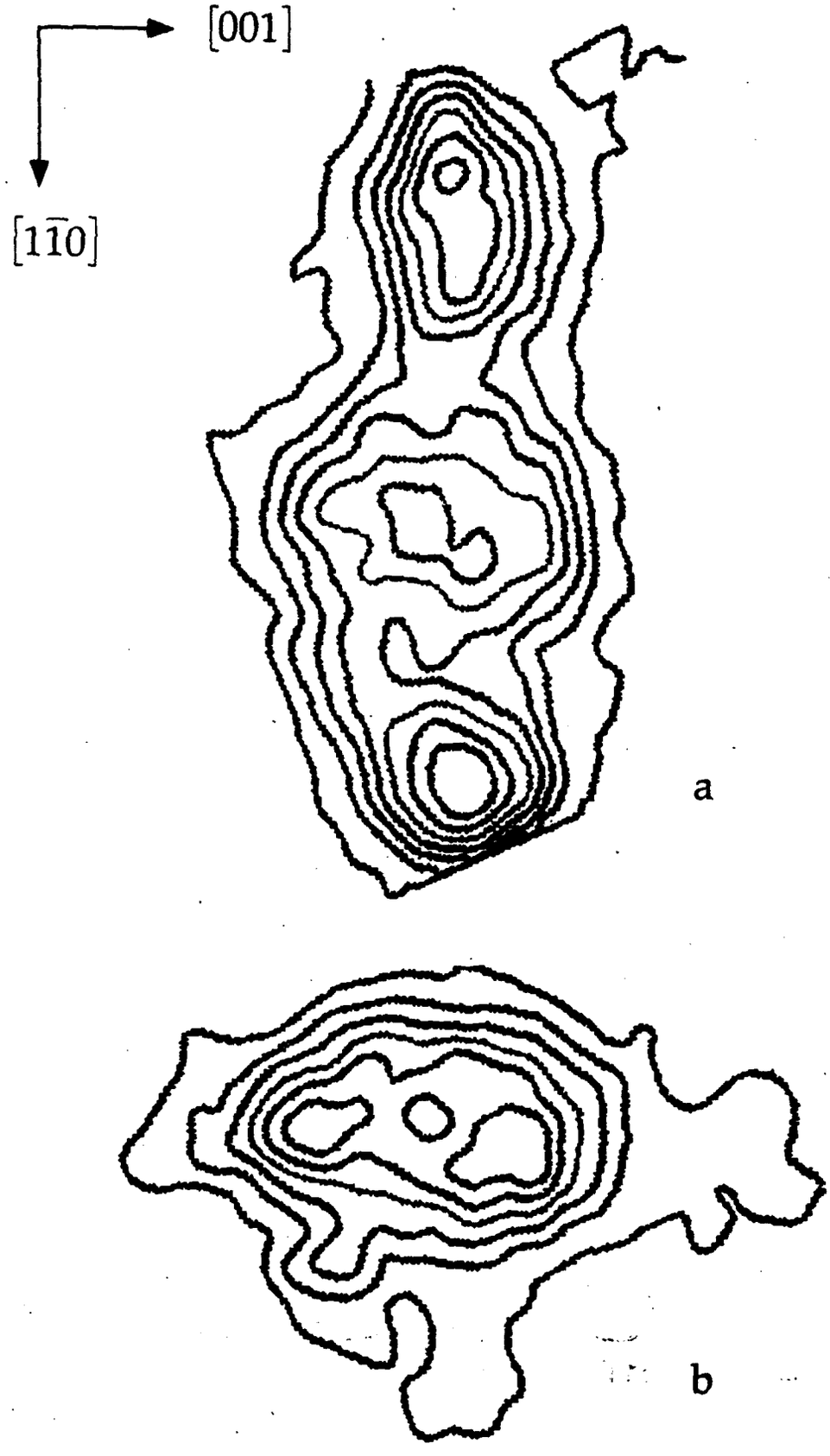

Fig. 4, Krasnopoler, Johnson, and Stuve

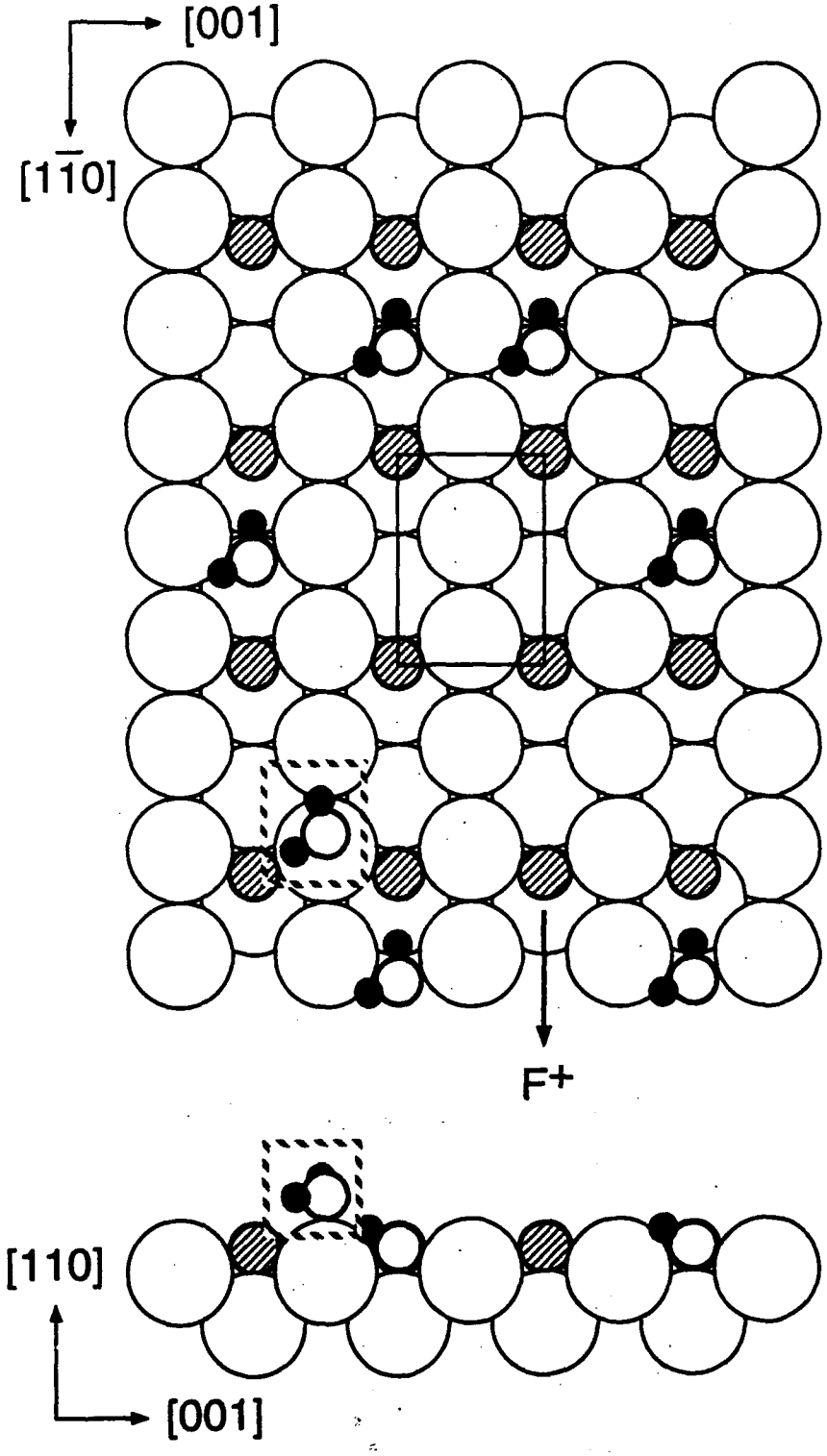

Fig. 5, Krasnopoler, Johnson, and Stuve

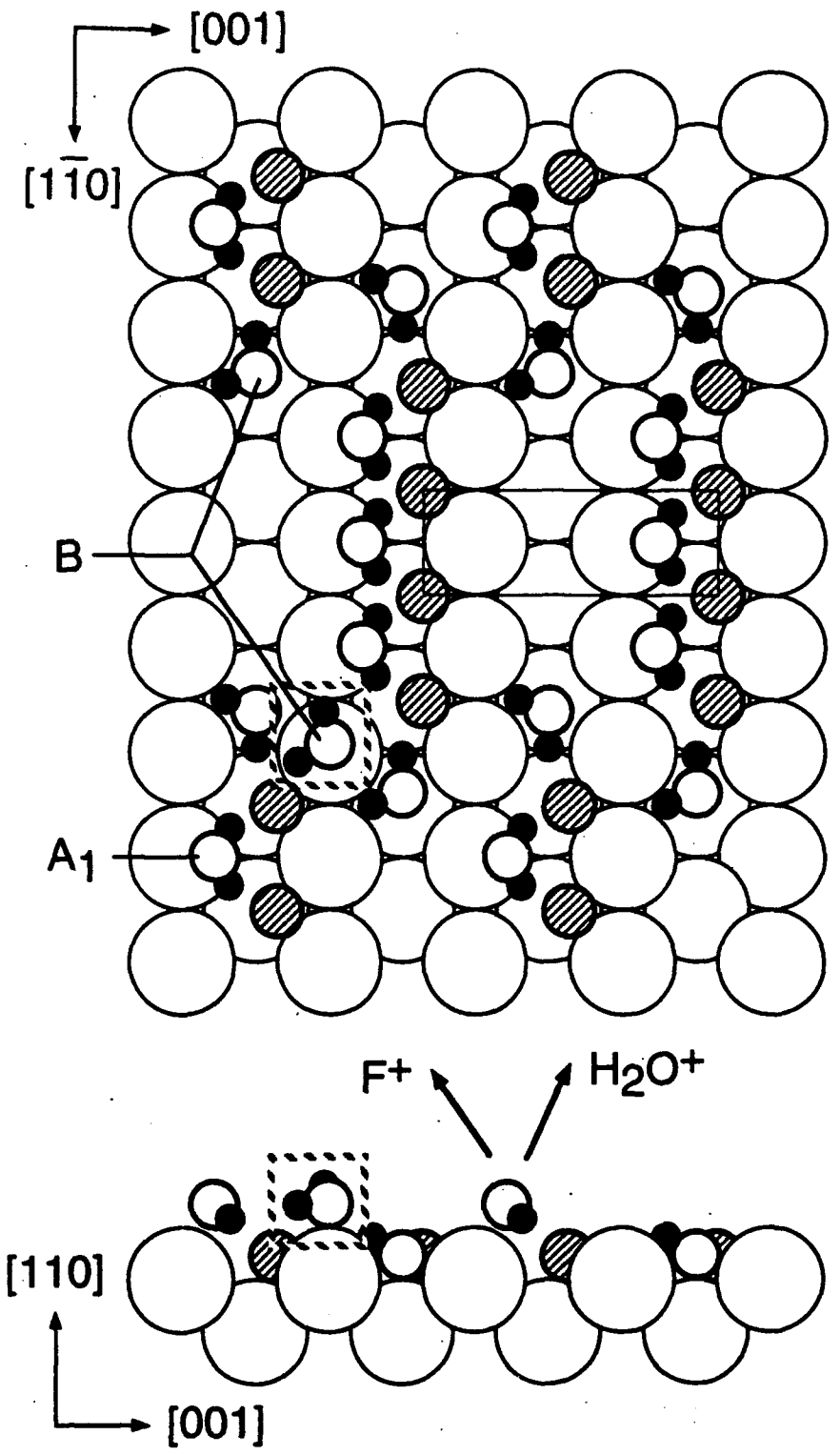

Fig. 6, Krasnopoler, Johnson, and Stuve